

RECORD OF WATER DEGASSING DURING MAGMA ASCENT. M. C. McCanta¹, M. D. Dyar², and E. Sklute², ¹Dept. of Earth & Planetary Sciences, University of Tennessee, 1621 Cumberland Ave, Knoxville, TN 37996 (mmccanta@utk.edu), ²Planetary Science Institute, 1700 East Fort Lowell, Tucson, AZ 85719.

Introduction: Saal et al. [1] measured H₂O in lunar picritic glass beads using SIMS at levels of ca. 10-50 ppm H₂O. These were the first direct measurements of volatiles in lunar glasses and diffusional modelling allowed for back-calculations that estimated 745 ppm H₂O (minimum 260 ppm) in their source region, suggesting a potentially “wet” lunar interior. These modelled levels of H₂O (and all other volatile species) are significantly higher than those in the as-erupted samples because volatile species are not stable in the melt phase under low pressure conditions [e.g., 2] and are therefore expected to have been lost during magma ascent and eruption (Fig. 1).

Moreover, there are differences in measured volatile concentrations (not corrected for diffusive loss during ascent and eruption) among very-low-Ti green glasses (>30 ppm H₂O), low-Ti green glasses (up to 46 ppm H₂O), and high-Ti orange glasses (>15 ppm H₂O) [1]. These results and analyses of melt inclusions in lunar olivine grains [3] suggest that volatiles may be heterogeneously distributed in the lunar interior.

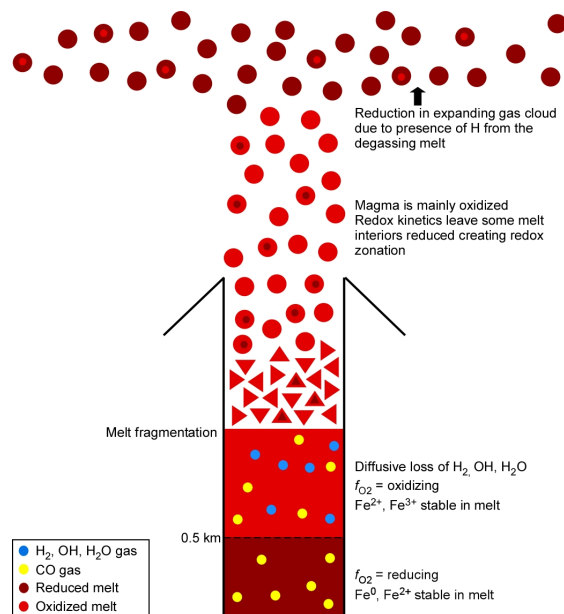


Figure 1. Oxidation/reduction environments in a melt column during ascent and eruption. From [4].

Background: Remote sensing provides macroscale observations of the lunar surface. Data from the Moon Mineralogy Mapper (M³) instrument on the Chandrayaan-1 spacecraft [5-6] have been used to identify “hydrous” surface deposits. These analyses required the additional step of attempting to isolate endogenous from exogenous water resulting from

solar wind implantation. Multiple potential candidate sites were identified across the lunar surface with estimated H₂O contents of up to 150 ppm for pyroclastic deposits and localized values of 300-400 ppm at some potential volcanic vent regions [5]. The heterogeneity of these H₂O concentrations is similar to that observed in the analytical works of [1,3]. However, *the total H₂O concentrations are significantly higher than those directly measured in the lunar glasses thought to be representative of the pyroclastic deposits* [1]. Additionally, high-Ti deposits have been observed [5] to be higher in H₂O than low-Ti, which was suggested to relate to faster cooling rates (i.e., less degassing) experienced by the high-Ti magmas. This conclusion is in direct contrast to the results of [1], where the high-Ti orange glasses contained almost no H₂O (>15 ppm) while the low-Ti green glasses had the most (up to 46 ppm). All glasses [1] contained significantly less H₂O than that estimated using M³ data. The high H₂O concentrations measured by [5-6] in ostensibly degassed deposits would imply significantly higher amounts of H₂O in the lunar interior. These remote measurements must be reconciled with high-resolution, Earth-based sample analysis.

Additional insight into melt (glass) H₂O concentration is provided by the oxidation state (recorded as oxygen fugacity: f_{O_2}) of the sample, as H and f_{O_2} are often correlated [e.g., 7]. For example, as water is diffusively lost (primarily as H₂ or OH) during magmatic degassing, the remaining system becomes more oxidizing [e.g., 8]. Therefore, quantifying the Fe³⁺/ΣFe of volcanic glasses may also provide important information regarding volatile degassing processes [e.g., 9].

Ideal terrestrial analogues for the lunar fire fountain eruptions are those observed at Kilauea volcano, Hawaii. Although magmatic and surface pressures and volatile contents and concentrations are quite different on Earth than the Moon, the basic geologic processes are similar (Fig. 1). Here we detail analytical work to constrain the H₂O diffusion and Fe³⁺ oxidation profiles in basaltic beads from Hawaiian fire fountain deposits to better constrain the changes that take place during ascent and eruption terrestrially. We then apply the results to lunar glass beads erupted under lunar conditions to determine the range of H₂O concentrations possible in pyroclastic deposits and compare that to remotely sensed values.

Samples and Methods: Volcanic glass beads from Kilauea volcano, Hawaii were provided by the

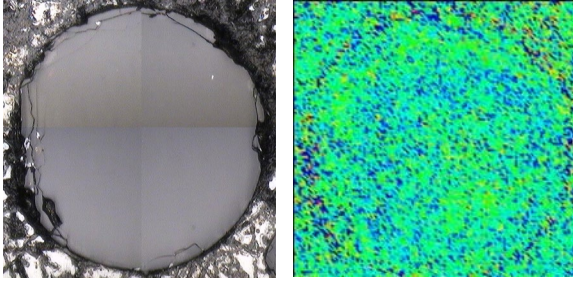


Figure 2. ATR micro-FTIR H map of glass bead (right, with photo at left) from Apollo 17 sample 74220, showing H gradients at the edge and interior.

Smithsonian Museum of Natural History. Beads were halved, placed in epoxy discs, and polished resulting in complete rim to rim cross sections. Additionally, several green glass beads from Apollo 15 and orange glass beads from Apollo 17 were analyzed.

Reflectance IR (ATR) determinations of H. Volcanic glass H concentrations were mapped *in situ* using reflectance FTIR at the University of Massachusetts on a Bruker Vertex 70 with a Hyperion 3000 microscope and an MCT focal plane array detector. H maps were created in OPUS using the area under the 3200-3500 cm^{-1} peak and known molar absorptivity coefficients. The ATR micro-FTIR technique, while less quantitative than transmission FTIR, allows the same polished surface to be used for 2D correlation maps and XAS redox studies. Both H and Fe^{3+} concentrations can thus be coregistered. FTIR was performed first to minimize the potential for beam damage.

X-ray absorption spectroscopy (XAS) determination of $\text{Fe}^{3+}/\Sigma\text{Fe}$. Redox ratios of glasses were analyzed *in situ* using spot sizes of ca. $1 \times 1 \mu\text{m}$ at the GSECARS X-ray Microprobe (13-ID-E) at the Advanced Photon Source at Argonne National Lab. Multivariate analytical methods [12] were used to predict the Fe^{3+} concentrations.

Results and Implications: Zonation in H concentration (Fig. 2) and $\text{Fe}^{3+}/\Sigma\text{Fe}$ (Fig. 3) was observed in multiple glass beads studied. This geochemical evidence of degassing is apparently retained in glass beads erupted under surface pressure conditions. The gradient from high H cores to low H rims is negatively correlated with the Fe^{3+} , which show low Fe^{3+} cores and high Fe^{3+} rims. This zonation is due to diffusional loss of H or OH, which would lead to more oxidizing environment. Because redox re-equilibration takes place rapidly [e.g., 9], melt redox could reset prior to cooling through the glass transition temperature.

Prior Hawaiian research indicates that melt inclusions and glasses from submarine eruptions (i.e., quenched at higher pressure) retain the most H_2O (up to 1 wt.%), while those from fire fountains erupted

under atmospheric pressure exhibit near-total degassing of H_2O , with maximum H_2O concentrations at the 1-bar solubility limit in basaltic melts [2]. This solubility limit would be significantly less on the Moon, where current atmospheric pressure is $\sim 3 \times 10^{-15}$ bars. Although models [10] suggest a short-lived atmospheric pressure of $\sim 9 \times 10^{-3}$ bars may have been sustained at 3.5 byr, this would only result in a maximum basaltic melt H_2O solubility of ~ 100 ppm using the data of [11]. This pressure-related solubility limit has critical implications for how much H_2O could reasonably be retained in basaltic melts erupted on the lunar surface for the majority of lunar history, regardless of the rapidity of cooling. *While the lowest remotely detected H_2O estimations may be feasible, H_2O values of hundreds of ppm are not possible.*

ATR micro-FTIR mapping of Hawaiian glass beads is ongoing to constrain degassing behavior. In addition, a new source of pristine lunar glass beads from unopened Apollo drill cores sampled as part of the ANGSA program, will provide new information on glass volatile concentrations at the lunar surface.

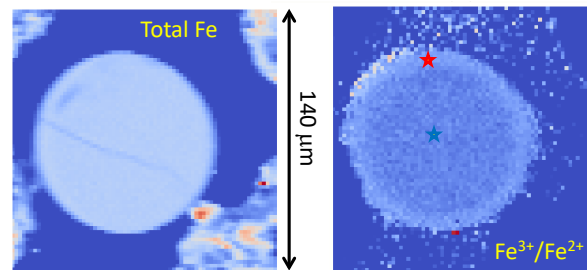


Figure 3. Apollo 11 lunar glass bead. XRF map of Fe $K\alpha$ (left) showing total Fe distribution in the bead and a map of calculated $\text{Fe}^{3+}/\text{Fe}^{2+}$ (right). For the total Fe map, dark blue areas show low Fe while white and red areas show high Fe. In the $\text{Fe}^{3+}/\text{Fe}^{2+}$ map, dark blue shows areas of low Fe^{3+} , with lighter shades of blue showing where Fe^{3+} contents are higher.

Acknowledgments: Supported by NASA grants NNX16AR18G (M.C.M) and 80NSSC19K0802 (M.D.D.).

References: [1] Saal et al. (2008) *Nature* 454, 192-196. [2] Wallace P. and Anderson A. T. (2000) in *Encyclopedia of Volcanoes*, 149-170. [3] Hauri et al. (2011) *Science* 333, 213-215. [4] McCanta M. C. et al. (2019) *Amer. Mineral.* 453-458. [5] Milliken R. E. and Li S. (2017) *Nature Geosci.* 10, 561-565. [6] Li S. and Milliken R. E. (2017) *Science Adv.* 3, e1701471. [7] Mysen B. et al. (2011) *GCA* 75, 6183-6199. [8] Christie D. M. (1986) *EPSL* 79, 397-411. [9] McCanta M. C. et al. (2017) *Icarus* 285, 95-102. [10] Needham D. H. and Kring D. A. (2017) *EPSL* 478, 175-178. [11] Newcombe M. E. (2017) *GCA* 200, 330-352. [12] Dyar et al. (2016) *Amer. Mineral.* 101, 744-748.